
NUCLEAR POTENTIALS FOR JOINT DESCRIPTION OF FEW-NUCLEON SYSTEMS AND STRUCTURE FUNCTIONS OF THREE-NUCLEON NUCLEI

D.V. PIATNYTSKYI, I.V. SIMENOG

UDC 539.172
© 2008

M.M. Bogolyubov Institute for Theoretical Physics, Nat. Acad. Sci. of Ukraine
(14b, Metrolohichna Str., Kyiv 03143, Ukraine; e-mail: ivsimenog@bitp.kiev.ua, dpyat@univ.kiev.ua)

For a satisfactory concordance of low-energy parameters for two nucleons and the energies of three- and four-nucleon nuclei, a version of the nucleon-nucleon potential is proposed. The construction scheme for such potentials is described. The precise calculations of the energies and radii of three- and four-nucleon nuclei are carried out using both the variational method with optimized Gaussian bases for different interaction potentials and the representation without isospin. The structure functions of T and ^3He nuclei are analyzed.

1. Introduction

The successes in study of few-nucleon problem owe to powerful variational methods, which give possibility to investigate bound states of few-nucleon systems, as well as few-nucleon scattering processes, and to study the finest structure of such systems [1–6]. The representation without isospin [4] can significantly reduce the number of independent equations for the spatial components of wave functions in few-nucleon problems, which greatly simplifies the calculations. Variational methods with Gaussian bases are very efficient and convenient for problems concerning few different particles, because the results for energy levels and corresponding wave functions can be obtained within these methods in a simple form with high accuracy.

The construction of nuclear interaction potentials to concord all the main characteristics such as binding energies, radii, structure functions, and low-energy scattering parameters for as many as possible nuclear systems is an important unsolved problem in nuclear theory. The presence of such nuclear potentials would allow to forecast more surely the

finest structure properties of the already existing and hypothetic nuclides, bounds of nuclear stability, and other fundamental characteristics. At present, there are many effective realistic potentials of interaction fitted by the large number of two-nucleon scattering data [7–9], which describe the energies and other parameters of three- and four-nucleon systems only in rather rough approximations. Even if one uses the simple two-parameter potentials, then it would be expected that few-nucleon nuclei will be sufficiently overbound in precise calculations. Thus, there are two outermost possibilities – simple potential models with the unsatisfactory description of complicated nuclei and awkward realistic models faced with the problem of reliable calculations. The development of prospective variational schemes of analysis of complicated many-body systems gives an opportunity to fill the available niche and to solve the problem of construction of realistic and yet simple NN-potentials, which could concord all the main low-energy few-nucleon parameters.

In the present work, the attempt of construction of a nucleon-nucleon interaction potential is carried out for the joint precise description of low-energy two-nucleon parameters, binding energies of a deuteron and three- and four-nucleon nuclei, and some structure functions. The general scheme of construction of such potentials is analyzed and a certain version of the potential is constructed. The bound-state energies, r.m.s radii of T, ^3He , and ^4He nuclei, density distributions, and formfactors are calculated with high precision. The analysis of the density distributions and formfactors for three-nucleon systems is carried out depending on properties of NN-potentials.

2. Statement of the Problem

Consider the ground states of three-nucleon nuclei ${}^3\text{He}$ (2p,n) and T (p,2n) with the two-nucleon central exchange potentials of interaction. The Hamiltonian of the system ${}^3\text{He}$ looks as

$$\hat{H} = \frac{1}{2m_p}(\hat{p}_1^2 + \hat{p}_2^2) + \frac{1}{2m_n}\hat{p}_3^2 + \sum_{i>j}^3 \hat{V}_{ij} + \frac{e^2}{|\vec{r}_1 - \vec{r}_2|}. \quad (1)$$

We take nuclear NN-potentials of interaction in the Majorana form

$$\hat{V}_{ij} = [V_s^+(r_{ij})\hat{P}_s(\sigma) + V_t^+(r_{ij})\hat{P}_t(\sigma)](1 + \hat{P}_r)/2 + [V_s^-(r_{ij})\hat{P}_s(\sigma) + V_t^-(r_{ij})\hat{P}_t(\sigma)](1 - \hat{P}_r)/2, \quad (2)$$

where \hat{P}_s and \hat{P}_t – spin operators in the singlet and triplet states of two nucleons, \hat{P}_r – the Majorana operator of permutation of the spatial nucleon coordinates, $V_{s,t}^\pm(r)$ – the singlet and triplet spherically symmetric NN-interaction potentials in even (+) and odd (-) states of the orbital moment.

For three-nucleon systems, we use the representation without isospin, where neutrons and protons are treated as different particles. The advantage of the representation without isospin is the essential simplification of the system of equations [4, 6] for the spatial components of the wave functions in comparison with the equivalent representation with isospin. Thus, for the concerned three-nucleon systems, we have two equations, whereas we have the systems of four spatial equations (T) and even of six equations for ${}^3\text{He}$ nucleus by using the isospin formalism. The representation without isospin gives possibility of achieving a high controllable accuracy. The total wave function of ${}^3\text{He}$ nucleus with spin $S = 1/2$ has the form

$$\Psi = \frac{1}{\sqrt{2}}(\zeta'\Phi_1 + \zeta''\Phi_2), \quad (3)$$

where ζ' and ζ'' are the components of the spin wave function for the doublet state $S = 1/2$ with the Young scheme [2,1], and the spatial components Φ_1 and Φ_2 are, respectively, symmetric and antisymmetric under the permutations of proton coordinates (1 \leftrightarrow 2). Similarly (3), we have the wave function for T nucleus

with the replacement of protons by neutrons. The system of equations for the spatial components of the wave function of ${}^3\text{He}$ nucleus in the framework of the representation without isospin has the form [4]

$$\begin{aligned} & [\hat{K} + \frac{e^2}{r_{12}} + V_{s(pp)}^+(r_{12}) - E]\Phi_1(123) + \\ & + \frac{1}{8} \sum_{ij=13,23} \sum_{+,-} [3V_{t(np)}^\pm(r_{ij}) + V_{s(np)}^\pm(r_{ij})] \times \\ & \times [1 \pm P(ij)]\Phi_1(123) + \\ & + \frac{\sqrt{3}}{8} \sum_{ij=13,23} \sum_{+,-} (-1)^{i+j} [V_{s(np)}^\pm(r_{ij}) - \\ & - V_{t(np)}^\pm(r_{ij})][1 \pm P(ij)]\Phi_2(123) = 0, \\ & [\hat{K} + \frac{e^2}{r_{12}} + V_{t(pp)}^-(r_{12}) - E]\Phi_2(123) + \\ & + \frac{1}{8} \sum_{ij=13,23} \sum_{+,-} [V_{t(np)}^\pm(r_{ij}) + 3V_{s(np)}^\pm(r_{ij})] \times \\ & \times [1 \pm P(ij)]\Phi_2(123) + \\ & + \frac{\sqrt{3}}{8} \sum_{ij=13,23} \sum_{+,-} (-1)^{i+j} [V_{s(np)}^\pm(r_{ij}) - \\ & - V_{t(np)}^\pm(r_{ij})][1 \pm P(ij)]\Phi_1(123) = 0. \end{aligned} \quad (4)$$

Here, \hat{K} is the kinetic energy of three nucleons, $\hat{P}(ij)$ – the permutation operator of spatial coordinates of nucleons with numbers i and j . For T (2n,p) nucleus with spin $S = 1/2$, the system of equations without isospin is similar, but it is necessary to permute indices $n \leftrightarrow p$ in every potential and to eliminate the Coulomb potential. It should be noted that the system of two equations (4) for the spatial functions is complete for the three-nucleon problem for bound states, as well as for scattering with the total spin $S = 1/2$ (doublet state).

3. Energy Matrix and Method of Calculation

Let us analyze the bound states of three-nucleon systems using the variational method with Gaussian bases. This method is convenient, because all matrix elements of Eq. (4) can be obtained in explicit form. Let's treat the spatial components of the variational wave function Φ_ν ($\nu = 1, 2$) with zero orbital moment for ${}^3\text{He}$ nucleus in the Gaussian basis as

$$\begin{aligned} \Phi_\nu &= \hat{S}_\nu \sum_{k=1}^{N_\nu} D_k^{(\nu)} \varphi_k^{(\nu)} \equiv \\ &\equiv \hat{S}_\nu \sum_{k=1}^{N_\nu} D_k^{(\nu)} \exp(-(a_k^{(\nu)} r_{12}^2 + b_k^{(\nu)} r_{13}^2 + c_k^{(\nu)} r_{23}^2)), \end{aligned} \quad (5)$$

where φ_ν are the Gaussian basis functions, N_ν – the basis dimension (N_1 for Φ_1 and N_2 for Φ_2), \hat{S} – the corresponding operator of symmetrization for the functions Φ_1 (symmetric) and Φ_2 (antisymmetric) relative to the permutation of identical protons ($1 \leftrightarrow 2$). Each basis function with zero moment depends on only three relative distances and has, respectively, three nonlinear variational parameters $a_k^{(\nu)}$, $b_k^{(\nu)}$, and $c_k^{(\nu)}$. With the use of the Gaussian basis, the energy matrix can be obtained in explicit form. The normalization for elementary (nonsymmetrized) basis functions has the form

$$\langle \varphi_k | \varphi_m \rangle = \frac{\pi^3}{3\sqrt{3}} \frac{1}{(a_{km} b_{km} + a_{km} c_{km} + b_{km} c_{km})^{3/2}},$$

$$a_{km} = a_k + a_m, b_{km} = b_k + b_m, c_{km} = c_k + c_m. \quad (6)$$

For convenience, we introduce the substitution

$$u_{12}^{km} \equiv a_k + a_m, u_{13}^{km} \equiv b_k + b_m, u_{23}^{km} \equiv c_k + c_m, \quad (7)$$

and

$$u_{12}^{km} u_{13}^{km} + u_{12}^{km} u_{23}^{km} + u_{13}^{km} u_{23}^{km} \equiv U_{km}. \quad (8)$$

Then (6) simplifies to

$$\langle \varphi_k | \varphi_m \rangle = \frac{\pi}{3\sqrt{3}} (U_{km})^{-3/2}. \quad (9)$$

In the present work, we only take the coordinate dependence of NN-potentials in the Gaussian form:

$$V(r_{ij}) = \sum_k V_{(0)k} \exp(-r_{ij}^2/r_{0k}^2). \quad (10)$$

Then the nonsymmetrized matrix element for one Gaussian component from (10) for the 1-st and 2-nd particles has the form

$$\begin{aligned} \langle \varphi_k | V(r_{12}) | \varphi_m \rangle &= \frac{\pi^3}{3\sqrt{3}} V_0 \times \\ &\times \left((u_{12}^{km} + \frac{1}{r_0^2}) (u_{13}^{km} + u_{23}^{km}) + u_{13}^{km} u_{23}^{km} \right)^{-3/2}, \end{aligned} \quad (11)$$

and the matrix elements for the other pairs of particles are similar just with the replacement of the corresponding numbering of particles.

The matrix element of the kinetic energy for three nucleons in the case where the masses of a proton and a neutron are equal has the form

$$\begin{aligned} \langle \varphi_k | K | \varphi_m \rangle &= \frac{\pi^3}{3\sqrt{3}} \frac{3\hbar^2}{2M} U_{km}^{-5/2} \times \\ &\times \left((4a_k a_m + a_k b_m + a_m b_k + a_k c_m + a_m c_k - \right. \\ &- b_k c_m - b_m c_k) (u_{13}^{km} + u_{23}^{km}) + \\ &+ (4b_k b_m + a_k b_m + a_m b_k + b_k c_m + b_m c_k - \\ &- a_k c_m - a_m c_k) (u_{12}^{km} + u_{23}^{km}) + \\ &+ (4c_k c_m + a_k c_m + a_m c_k + b_k c_m + b_m c_k - \\ &\left. - a_k b_m - a_m b_k) (u_{12}^{km} + u_{13}^{km}) \right). \end{aligned} \quad (12)$$

In its turn, the matrix element for the Coulomb potential has the form

$$\langle \varphi_k | \frac{e^2}{r_{12}} | \varphi_m \rangle = \frac{\pi^3}{3\sqrt{3}} \frac{2e^2}{(U_{km} \sqrt{u_{13}^{km} + u_{23}^{km}})}. \quad (13)$$

Having the energy matrix, one can determine the bound states in the variational Galerkin method by solving the linear algebraic system for expansion coefficients $D_n^{(\nu)}$ of the total spatial functions (5) in the Gaussian basis:

$$\begin{aligned} &\sum_{n=1}^{N_1} (\langle \hat{S} \varphi_m^{(1)} | \hat{H}_{11} | \hat{S} \varphi_n^{(1)} \rangle - E \langle \hat{S} \varphi_m^{(1)} | \hat{S} \varphi_n^{(1)} \rangle) D_n^{(1)} + \\ &+ \sum_{n=1}^{N_2} \langle \hat{S} \varphi_m^{(1)} | \hat{H}_{12} | \hat{S} \varphi_n^{(2)} \rangle = 0, \\ &\sum_{n=1}^{N_1} \langle \hat{S} \varphi_k^{(2)} | \hat{H}_{21} | \hat{S} \varphi_n^{(1)} \rangle + \end{aligned}$$

$$+ \sum_{n=1}^{N_2} (\langle \hat{S}\varphi_k^{(2)} | \hat{H}_{22} | \hat{S}\varphi_n^{(2)} \rangle - E \langle \hat{S}\varphi_k^{(2)} | \hat{S}\varphi_n^{(2)} \rangle) D_n^{(2)} = 0,$$

$$m = 1, 2, \dots, N_1; k = 1, 2, \dots, N_2. \quad (14)$$

Here, the operator block \hat{H}_{11} corresponds to the diagonal transitions between symmetrized basis functions $|\hat{S}\varphi_n^{(1)}\rangle$ (and symmetrized total spatial functions Φ_1), the block \hat{H}_{22} – the diagonal transitions between antisymmetrized basis functions $|\hat{S}\varphi_n^{(2)}\rangle$ (and antisymmetrized functions Φ_2), and the blocks \hat{H}_{12} and \hat{H}_{21} correspond to the nondiagonal transitions between functions of different symmetries. From the system of linear algebraic equations (14) for the possible energies of bound states (which can be obtained from the equality of the determinant of the energy matrix to zero), one can find the linear coefficients $D_n^{(\nu)}$ (state vectors) and the total wave functions in the form of a Gaussian superposition. We note that the linear coefficients $D_n^{(\nu)}$ together with other nonlinear parameters $a_k^{(\nu)}$, $b_k^{(\nu)}$, and $c_k^{(\nu)}$ play the role of variational parameters in case of using the straight variational Ritz principle.

The calculation of the variational parameters from the condition of reaching the lowest value of the ground-state energy with large bases can be a complicated task (see [10]). In the present work on some stages of precise calculations, we use the Ritz method along with the system of equations in the Galerkin method (14) with the optimization of the Gaussian bases by nonlinear parameters to quicken the calculations with large bases. The optimal scheme is to use alternately the variational schemes of Galerkin and Ritz.

There is the fundamental problem of optimization by nonlinear parameters for obtaining a high controlled accuracy in variational calculations. In the present work, we combine efficiently the stochastic methods of optimization (on the initial stage of optimization) with the regular methods of minimization by separate groups of parameters. Such an approach to the optimization of the Gaussian basis allows to obtain results for few-nucleon systems with high accuracy even for sufficiently small dimensions of the basis.

4. The Peculiarities of Construction of a Nuclear Potential for the Joint Description of Few-Nucleon Nuclei

The possibility of construction of a NN-potential for the simultaneous description of all the main parameters

of the few-nucleon systems is realized here. The two-nucleon scattering phase-shifts and the low-energy scattering parameters (scattering lengths and effective interaction radii) are calculated with the use of the variable phase approach [11]. The bound state of a deuteron is calculated by using the standard difference methods, as well as the variational method. We calculated the bound states of three- and four-nucleon systems with the help of the variational schemes mentioned above.

Our general purpose is to construct NN-potentials which can concord the low-energy characteristics of few-nucleon systems such as the two-nucleon scattering lengths and the ground-state energies of a deuteron and T, ^3He , ^4He nuclei. Two ways are used: in the first way, the potentials with spare parameters are fitted to some two-nucleon parameters and then the free (spare) parameters are used to describe the bound states of three- and four-nucleon systems; in the second, the two-, three- and four-nucleon data are fitted simultaneously. The standard schemes of potential construction are different: the realistic potentials with complex form are constructed at first to concord the two-nucleon phase-shifts, and then they are used for more complicated systems. In our work, we use the idea of the simultaneous description of main characteristics of two-, three- and four-nucleon systems without preference for the two-nucleon problem.

Let us consider at first the simplest variant of charge-independent potentials of nuclear interaction in the triplet and singlet states in the form of one-component attractive Gaussoids. Let's carry out the ground-state energy calculations in the simplest approximation (5) using the basis of three symmetric ($N_1 = 3$) and one antisymmetric ($N_2 = 1$) functions for economy. The potentials in the singlet and triplet states of two nucleons,

$$V_s(r) = -V_{0s}e^{-\left(\frac{r}{r_s}\right)^2}, \quad V_t(r) = -V_{0t}e^{-\left(\frac{r}{r_t}\right)^2}, \quad (15)$$

have two parameters – the attractive intensities and the interaction radii. Let's describe the experimental value of the np-scattering length in the singlet state a_s and the deuteron's ground-state energy ε_d in the triplet state with the use of the intensities of potentials (15) with fixed radii $r_{s,t}$. Then, in each state (s and t), we have radii as free parameters (one at each state) which are used to fit the experimental value of the triton binding energy ε_T . Then, with a fixed triton binding energy, we

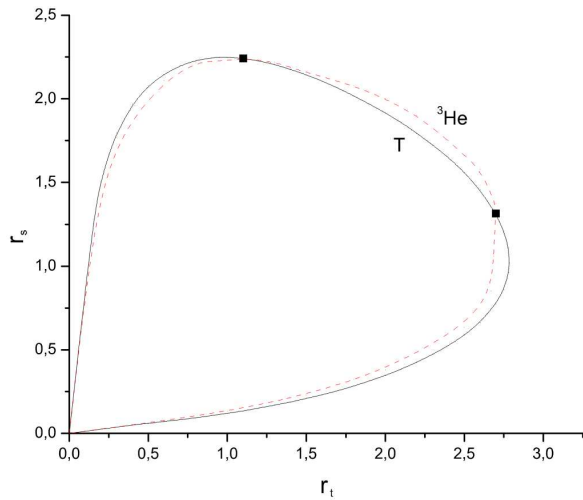


Fig. 1. Radius of the singlet potential versus the radius of the triplet potential at fixed $\varepsilon(T) = 8.481$ MeV, $\varepsilon(^3\text{He}) = 7.718$ MeV, $\varepsilon_d = 2.224575$ MeV, $a_s = -23.748$ fm

have the one-parameter group of two-nucleon potentials (the T -curve in Fig. 1), when the radii of the singlet and triplet potentials are connected (dependence $r_s(r_t)$). In Fig. 1, the potential radii are measured in fm (further, all lengths are measured in fm, energies in MeV; moreover, $\frac{\hbar^2}{m} = 41.47 \text{ MeV} \cdot \text{fm}^2$). This isoenergy curve encloses at zero, when the interaction radii are very small, and the intensities are large ($V_{0s,t} \approx \frac{\text{const}}{r_{s,t}^2}$). The points inside the closed isoenergy curve for T suit the potentials which overbind a T nucleus, the points outside the curve – underbind a triton. Since, for the fixed large value of binding energy of a T nucleus, the isoenergy curve passes near very small potential radii, this reflects the well-known fact of the existence of a collapse in the system of three particles with zero interaction radii (the Thomas effect). In a similar manner, the isoenergy curve of ^3He suits the fixed binding energy of ^3He nucleus. Moreover, in the case of small radii of nuclear interaction, the Coulomb interaction becomes efficiently suppressed, and curves for T and ^3He are close to each other. The isoenergy curves for T and ^3He nuclei cross at two points (marked by squares in Fig. 1), and we have two versions of potentials which concord the binding energies of T and ^3He nuclei (along with the fixed binding energy of a deuteron and the np-scattering length in the singlet state). These two potentials have the form

$$\begin{aligned} 1) V_s(r) &= -20,01e^{-\left(\frac{r}{2.242}\right)^2}, & V_t(r) &= -120.42e^{-\left(\frac{r}{1.1}\right)^2}, \\ 2) V_s(r) &= -60,59e^{-\left(\frac{r}{1.315}\right)^2}, & V_t(r) &= -28.15e^{-\left(\frac{r}{2.7}\right)^2}. \end{aligned} \quad (16)$$

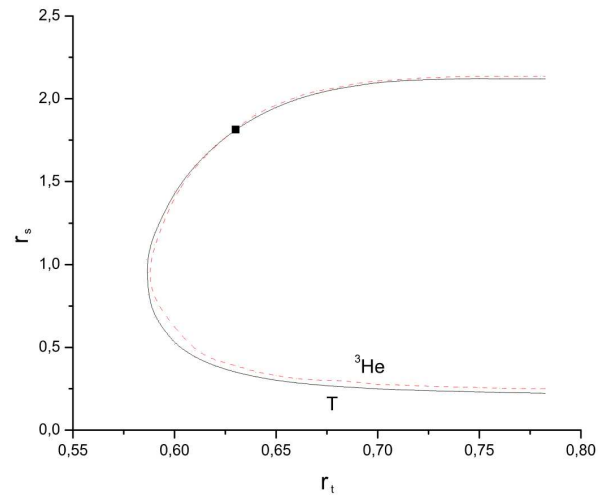


Fig. 2. Radius of the singlet potential versus the radius of the triplet potential at fixed $\varepsilon(T) = 8.481$ MeV, $\varepsilon(^3\text{He}) = 7.718$ MeV, $\varepsilon_d = 2.224575$ MeV, $a_s = -23.748$ fm, $a_t = 5.424$ fm

It should be noted that the first version of potential is more preferable, because the triplet radius must be smaller than the singlet radius. The obtained potentials (16) are dependent of the description accuracy of three-nucleon systems. In the case of a more accurate calculation of three-nucleon systems, it is expected that the situation will remain qualitatively the same – there will be two versions of potentials which could describe simultaneously the binding energies of two three-nucleon nuclei.

Let us consider now the description of the binding energy of alpha-particle ($\varepsilon_{4\text{He}} = 28.3$) together with energy of T (or ^3He). In rough approximations of three- and four-nucleon energy calculations ($N_1 = 3$ and $N_2 = 1$) with two parameters (the interaction radii in triplet and singlet states), one fails to exactly describe two values (binding energies of T and ^4He), and the corresponding isoenergy curves do not intersect. On isocurves for three-nucleon nuclei, the values of binding energies for four nucleons are always greater than the experimental ones. In Fig. 1, the isocurve for ^4He always lies outside the isocurves for three nucleons. Moreover, the intersection between isocurves for three and four nucleons is possible only when the binding energy of four nucleons is slightly greater than 30.1 MeV. When the more precise calculations are performed for binding energies of three- and four-nucleon systems, the isoenergy curves in Fig. 1 would cover larger regions, but their intersection is improbable.

It is interesting to consider a more complicated form of the triplet potential with two Gaussian components

in (10) taking the short-range repulsion into account. Let's bring three parameters into this potential – two intensities (attraction and repulsion) and one interaction radius with a fixed connection between repulsion and attraction radii

$$V_s(r) = -V_{0s}e^{-\left(\frac{r}{r_s}\right)^2},$$

$$V_t(r) = V_{0t}^{(1)}e^{-\left(\frac{r}{r_t}\right)^2} - V_{0t}^{(2)}e^{-\left(\frac{r}{2r_t}\right)^2}. \quad (17)$$

We fit again the singlet potential (its intensity) to the experimental value of scattering length, the triplet potential (two intensities) to both the binding energy of a deuteron and the scattering length in the triplet state. The radii of the singlet and triplet potentials are used to fit the values of the binding energies of T and ${}^3\text{He}$ ($N_1 = 3$ and $N_2 = 1$). The isoenergy curves (Fig. 2) have different forms, because of a repulsion in the triplet potential – there is no short radius region. In Fig. 2, we do not go beyond the region, where the radii of potentials have no sense. The point of intersection of the isoenergy curves for triton and ${}^3\text{He}$ is indicated in Fig. 2. In this case, there is one version of the potential that simultaneously describes the experimental values of scattering lengths in the singlet and triplet states and the binding energies of deuteron, triton, and ${}^3\text{He}$. This potential has the form

$$V_s(r) = -31.11e^{-\left(\frac{r}{1.815}\right)^2}.$$

$$V_t(r) = 330.0e^{-\left(\frac{r}{0.63}\right)^2} - 160.54e^{-\left(\frac{r}{1.26}\right)^2}. \quad (18)$$

It is quite similar to the standard nucleon-nucleon potentials. We note that, in case of potentials (18), the isoenergy curve for ${}^4\text{He}$ is situated outside three-nucleon curves – the energies of the three-nucleon systems and the four-nucleon system are incompatible again.

Above, we have presented the examples of construction of simple potentials for the description of bound states in a rough approximation. From these examples, some general rules of the potential construction can be seen. When we take potentials in a more complicated form and use a higher accuracy in calculations, the general scheme of potential construction remains mainly the same. In this case, it is reasonable to fit the parameters for physical values on the average (not exactly) with the minimization of root-mean-square deviations. Such potentials in different two-nucleon states were built with regard for two Gaussian components in (10) and were used in the precise calculations of few-nucleon systems (let us call

this potential K2; do not mix it up with an analogous notation in [10]):

$$V_{s(nn)}(r) = 817.0 \exp\left(-\left(\frac{r}{0.63}\right)^2\right) - 206.34 \exp\left(-\left(\frac{r}{1.18}\right)^2\right).$$

$$V_{s(pp)}(r) = 490.0 \exp\left(-\left(\frac{r}{0.68}\right)^2\right) - 151.07 \exp\left(-\left(\frac{r}{1.27}\right)^2\right).$$

$$V_{s(np)}(r) = 3950.0 \exp\left(-\left(\frac{r}{0.55}\right)^2\right) - 381.38 \exp\left(-\left(\frac{r}{1.1}\right)^2\right).$$

$$V_{t(np)}(r) = 3720.0 \exp\left(-\left(\frac{r}{0.488}\right)^2\right) - 528.59 \exp\left(-\left(\frac{r}{0.976}\right)^2\right). \quad (19)$$

All potentials have the short-range repulsive part and the attractive one at longer distances. We divide the singlet potential V_s into three singlet potentials ($V_{s(nn)}$, $V_{s(pp)}$, and $V_{s(np)}$) respectively to the nucleon pairs nn, pp, and np, because it was possible to describe the Coulomb energy (adjust the binding energies of triton and ${}^3\text{He}$) only in such way. These singlet potentials are fitted to experimental values of the nn, pp, and np scattering lengths. The triplet potential was fitted to both the scattering length in the triplet state and the deuteron binding energy. The experimental values for scattering lengths and effective radii of interaction are as follows (all lengths are measured in fm, energies – MeV) [12]: $a_{t(np)} = 5.419 \pm 0.007$, $a_{s(np)} = -23.740 \pm 0.02$, $a_{s(nn)} = -18.9 \pm 0.4$, $a_{s(pp)} = -17.3 \pm 0.4$ (without Coulomb); $r_{0t(np)} = 1.753 \pm 0.008$, $r_{0s(np)} = 2.77 \pm 0.05$, $r_{0s(nn)} = 2.75 \pm 0.11$, $r_{0s(pp)} = 2.85 \pm 0.04$. Potential (19) gives the following values of two-nucleon low-energy parameters: $E_D = -2.2248$, $a_{t(np)} = 5.424$, $a_{s(np)} = -23.746$, $a_{s(nn)} = -18.904$, $a_{s(pp)} = -17.308$, $r_{0t(np)} = 1.785$, $r_{0s(np)} = 2.752$, $r_{0s(nn)} = 2.594$, $r_{0s(pp)} = 2.670$.

In the previous work [6], we already tried to build a charge independent nucleon-nucleon potential in a simple form for the precise description of the main

parameters of few-nucleon nuclei. As a result, potential K1 was obtained in the form

$$V_s(r) = -27.38e^{-\left(\frac{r}{1.93}\right)^2},$$

$$V_t(r) = 23789.46e^{-\left(\frac{r}{0.42}\right)^2} - 1169.92e^{-\left(\frac{r}{0.85}\right)^2}. \quad (20)$$

This potential is built to fit experimental values of the deuteron binding energy and scattering lengths in the triplet and singlet states. Potential (20) gives the following values for the energies of three- and four-nucleon nuclei:

$$\varepsilon_T = 8.467, \quad \varepsilon_{^3\text{He}} = 7.758, \quad \varepsilon_{^4\text{He}} = 28.60.$$

Potential (20) gives worse results, on the average, for the energies of few-nucleon systems than the new version K2 (19). Moreover, the K1 potential in the triplet state has large intensities, which produces the certain difficulties in precise calculations of few-nucleon nuclei.

Let us return to the K2 potential (19). We note that this potential fits well the experimental values of scattering lengths. For the effective radii of interaction, it gives slightly worse results. We rejected the precise description of experimental values of the effective radii of interaction in favor of a more accurate description of the binding energies of T, ^3He , ^4He nuclei. The typical example for the triplet phase-shifts with the K2 potential is presented in Fig. 3, where one can see the degree of agreement with experimental data [12].

Let us consider some calculational problems for the binding energies and radii of few-nucleon systems using potential (19). During the calculations of the ground-state energies for T, ^3He , and ^4He nuclei, it is determined that the symmetric component of the coordinate function Φ_1 makes the main contribution to the energy. The antisymmetric component Φ_2 makes a

Table 1. Binding energies of T, ^3He , ^4He nuclei for potentials K2, Minnesota(M), Afnan-Tang(AT⁺) and K1

Potentials	$E(\text{T})$	$E(^3\text{He})$	$E(^4\text{He})$
K2	-8.475	-7.691	-28.298
M	-8.389 [6]	-7.712 [6]	-29.948 [6]
AT ⁺	-8.494 [6]	-7.836 [6]	-29.733 [6]
K1	-8.467 [6]	-7.758 [6]	-28.60 [6]
Experiment	-8.482	-7.718	-28.296

Table 2. R.m.s. radii of T and ^3He nuclei – proton R_p , neutron R_n , mass R_m

Potentials	$R_p(\text{T})$	$R_n(\text{T})$	$R_m(\text{T})$	$R_p(^3\text{He})$	$R_n(^3\text{He})$	$R_m(^3\text{He})$	Ref.
K2	1.613	1.769	1.718	1.814	1.636	1.757	Our work
M	1.586	1.736	1.706	1.798	1.604	1.736	[6]
AT ⁺	1.575	1.746	1.691	1.778	1.591	1.718	[6]
K1	1.602	1.758	1.708	1.794	1.621	1.738	[6]

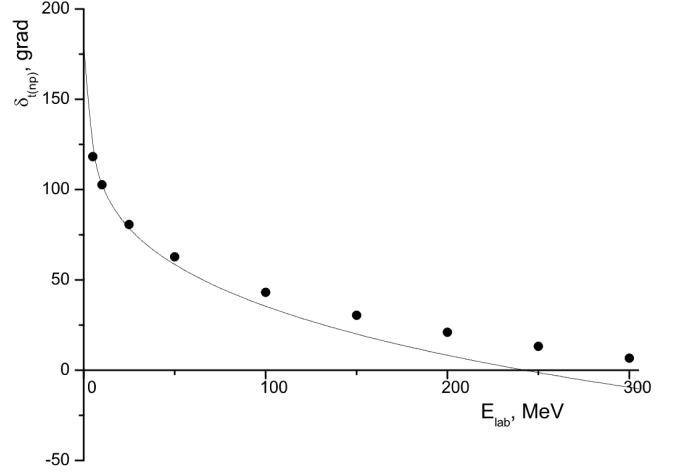


Fig. 3. Triplet phase shift for the K2 potential (dots – experimental data)

noticeably less contribution. Therefore, it is appropriate to represent accurately the symmetric function during the expansion of the coordinate function in the Gaussian basis. The optimal ratio between the numbers of basis function components is 2.5 (in (5) $N_1 \approx 2.5N_2$). Generally, one should take two or three hundreds of basis functions to gain a precise result. If the potential contains an essential repulsion, then it is necessary to use a greater dimension of the basis in order that the wave function could reproduce a more drastic change of regimes depending on distance.

The neutron, proton, and mass density distributions, the r.m.s. radii of these distributions, and the formfactors of three-nucleon nuclei are calculated with help of the precise and simple variational wave functions (5). The binding energies for the K2 potential and three other potentials known from the literature are presented in Table 1 together with experimental data [13].

One could see that the K2 potential gives sufficiently good results for the binding energies of three- and four-nucleon nuclei in comparison with other potentials. The Minnesota (M) potential gives the most unsatisfactory results for three-nucleon nuclei and for ^4He [6]. The K1 and K2 potentials give values of the binding energies of an alpha-particle close to experimental ones, whereas the

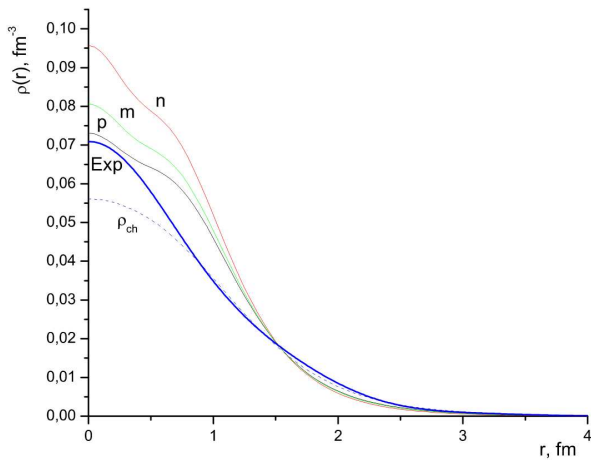


Fig. 4. Density distributions for ${}^3\text{He}$ using the K2 potential (Exp – experimental data, p – proton, n – neutron, m – mass, the dotted line – charge distribution taking into account non-point nucleons)

Minnesota and Afnan–Tang potentials (AT^+) overbind this nucleus. The K2 potential gives also the value of Coulomb energy close to the experimental one $E_C = E({}^3\text{He}) - E(\text{T}) = 0.784$ (experimental value $E_C = 0.765$), whereas this is traditionally the significant problem even for more complicated forms of potentials. The results for the radii (when nucleons are point-like) of T and ${}^3\text{He}$ nuclei are presented in Table 2.

The K2 potential gives the following values of r.m.s. radii for ${}^4\text{He}$: $R_p = 1.494$, $R_n = 1.488$, $R_m = 1.491$. The values of r.m.s. radii for three-nucleon nuclei calculated for the K2 potential are slightly bigger than the others, because the K2 potential has considerable short-range repulsion.

For comparison with the experimental values of r.m.s. charge radii, the transition from proton radii (point-like nucleons) to charge radii (non-point nucleons) should be made with the help of the simple formula [14]

$$\langle R_{\text{ch}}^2 \rangle = \langle R_p^2 \rangle + \langle r_p^2 \rangle + \frac{N}{Z} \langle r_n^2 \rangle. \quad (21)$$

Here, $r_p = 0.811$ Fm, and the hypothetical value $r_n^2 = -0.2$ Fm 2 . For three-nucleon nuclei, we get the results: $R_{\text{ch}}(\text{T}) = 1.613$ Fm, $R_{\text{ch}}({}^3\text{He}) = 1.961$ Fm. These values are close to the experimental charge radii which were obtained by different authors, for example, $R_{\text{ch}}^{\text{exp}}(\text{T}) = (1.70 \pm 0.05)$ Fm [15], $R_{\text{ch}}^{\text{exp}}({}^3\text{He}) = (1.976 \pm 0.013)$ Fm [16] (see also [17–21]). Thus, one can see that the K2 potential gives sufficiently good qualitative results for r.m.s. charge radii of T, ${}^3\text{He}$ nuclei. It can be seen from Table 2 that, in particular, the r.m.s. proton radius

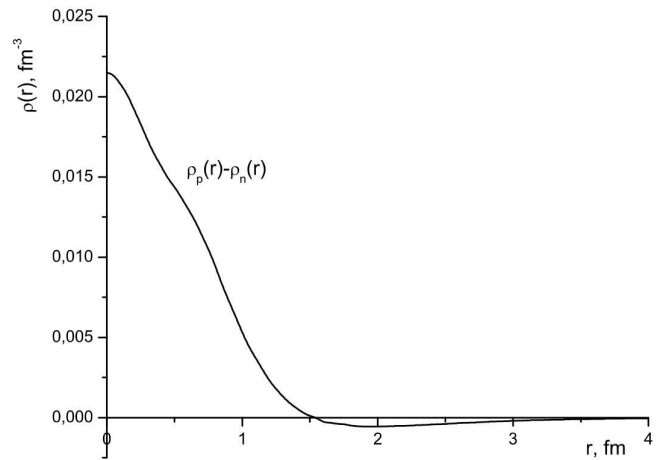


Fig. 5. Difference between the density distributions of protons and neutrons in a T nucleus

of ${}^3\text{He}$ nucleus is bigger than r.m.s. neutron radius, because of the Coulomb repulsion between protons. On the contrary, for T nucleus, the proton radius is lesser than the neutron radius. This can be explained mainly by the fact that the K2 potential has weaker attraction between identical nucleons (neutron-neutron, proton-proton) than that between a neutron and a proton.

5. Density Distributions for Three-nucleon Systems

The variational method with a Gaussian basis allows one to obtain the wave functions in a convenient form. Let us determine the proton density distribution for ${}^3\text{He}$ as

$$\rho_p(r) = \langle \Psi | \frac{1}{2} \sum_{i=1}^2 \delta(\vec{r} - (\vec{r}_i - \vec{R}_{\text{c.m}})) | \Psi \rangle. \quad (22)$$

In the mass density distribution, there is a sum over all nucleons, and, in the neutron distribution, only the third particle (neutron) is taken into account. Here, the wave function is normalized to unity, and $\vec{R}_{\text{c.m}}$ is the center-of-mass coordinate. The density distributions for a T nucleus are analogous.

The proton, neutron, and mass density distributions for ${}^3\text{He}$ (point-like nucleons) and the charge distribution ρ_{ch} (for non-point nucleons), which are calculated using the K2 potential, and the “experimental” charge distribution [17] are represented in Fig. 4. We note that some irregularity in the short-range behavior of the density distributions is a consequence of the presence of the essential repulsion in the K2 potential (especially

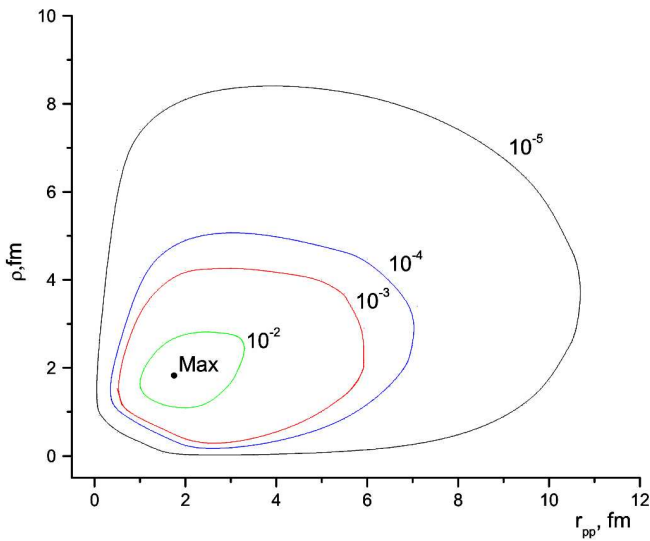


Fig. 6. Isolines of the density distribution in ${}^3\text{He}$ nucleus – function $R(r_{pp}, \rho) = \text{const}$

that between a neutron and a proton in the singlet and triplet potentials). If we modify the potentials, then such an irregularity in the density distribution disappears with decrease in the repulsion (the curves become “smoother”). It should be mentioned that the “experimental” curve for the charge density distribution is obtained by the Fourier transformation of the experimental formfactor in [17]) and has no such irregularities. If we take into account non-point nucleons, then the irregularity in the density distributions calculated by us disappears, and the curve for the charge distribution descends lower. The curve for the neutron distribution at short distances lies higher than the curve for the proton distribution. At larger distances, the curve for protons in ${}^3\text{He}$ lies higher because of the Coulomb repulsion. In the case of a T nucleus, the proton, neutron, and mass density distributions together with oscillations repeat the behavior of the density distributions for ${}^3\text{He}$ (the proton density for T lies close to the neutron density of ${}^3\text{He}$, and the neutron density for T – to the proton density of ${}^3\text{He}$). The difference between the proton and neutron densities for a triton nucleus is shown in Fig. 5. The difference of densities in minimum makes one percent of the absolute value of the distribution.

Let us consider also the function of the density $R(r_{pp}, \rho)$ for a ${}^3\text{He}$ nucleus (for a T nucleus, it will be $R(r_{nn}, \rho)$)

$$R(r_{pp}, \rho) = r_{pp}^2 \rho^2 \langle |\Psi(r_{pp}, \rho, \theta)|^2 \rangle_{\theta}, \quad (23)$$

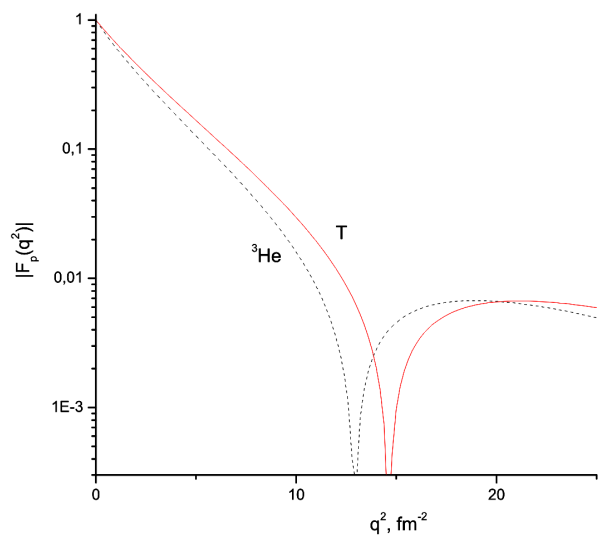


Fig. 7. Proton formfactors of three-nucleon nuclei for the K2 potential (point-like nucleons)

where we carried out the averaging of the squared full three-particle wave function of a ${}^3\text{He}$ system by the angle between the relative Jacobi coordinate \vec{r}_{pp} and the vector $\vec{\rho}$ that means the distance from a neutron to the center of mass of two protons (analogously for a T nucleus with replacement of protons to neutrons) and the distance from the center of mass to the third particle. Function (23) defines the possibility of a structure arrangement of two protons and neutron in a ${}^3\text{He}$ nucleus. In Fig. 6 for a ${}^3\text{He}$ nucleus, the curves of r_{pp} versus ρ are built at fixed values of the density function $R(r_{pp}, \rho)$ (isolines of density averaged over the angle). These curves are the expected ellipse-like curves with one center, where the density $R(r_{pp}, \rho)$ has its maximum value, and this is a convenient arrangement (correlation between the distances r_{pp} and ρ) that is close to an equilateral triangle for the system of three almost equivalent nucleons. The analogous structure is typical of a T nucleus (protons are replaced by neutrons).

6. Formfactor Properties

Let us consider the formfactors of three-nucleon systems, particularly, the charge formfactor

$$F_p(q^2) = \int \rho_p(r) \exp(-i(\vec{q}\vec{r})) d\vec{r}. \quad (24)$$

The neutron and mass formfactors are determined analogously as the Fourier transform of the corresponding density distributions. We note that definition (24) corresponds to the approximation of

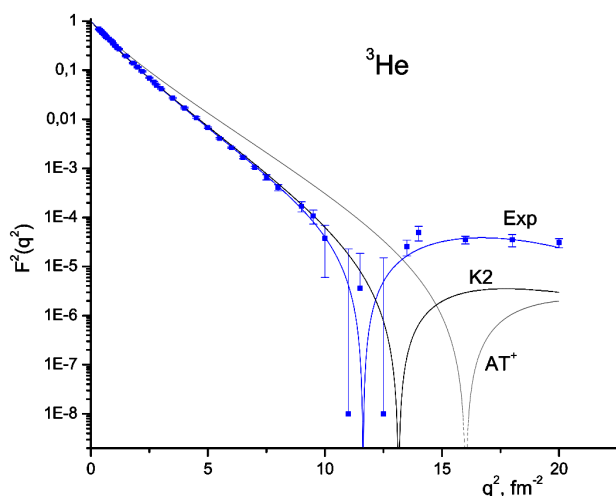


Fig. 8. Charge form factors in a ${}^3\text{He}$ nucleus for the potentials K2 and AT^+ (dots – experimental data)

structureless point-like nucleons (non-point nucleons will be considered in what follows). The behavior of the proton formfactors for ${}^3\text{He}$ and T nuclei as functions of the square momentum transfer q^2 is shown in Fig. 7. The formfactor for a ${}^3\text{He}$ nucleus for small q^2 decreases faster, because the proton r.m.s. radius in a ${}^3\text{He}$ nucleus is bigger than the proton r.m.s. radius of a T nucleus. Moreover, the “dip” in the formfactor for a ${}^3\text{He}$ nucleus is shifted essentially towards smaller transferred momenta. For charge formfactors, let us consider non-point nucleons. This can be done using the well-known formula [10, 22]

$$F_{\text{ch}} = F_p f_p + \frac{N}{Z} F_n f_n, \quad (25)$$

where we use the following parametrization for the formfactors of individual protons and neutrons f_p and f_n : $f_p = (1 + \frac{1}{12}q^2 r_p^2)^{-2}$ and $f_n = (1 + \frac{1}{12}q^2(r_p - 0.06)^2)^{-2} - (1 + \frac{1}{12}q^2(r_p + 0.06)^2)^{-2}$, where $r_p = 0.811$ fm is the r.m.s. radius of the proton. The results of calculations show that the neutron part gives a small contribution to the formfactor as compared with the proton part and, therefore, it can be neglected.

The behavior of the charge formfactor of a ${}^3\text{He}$ nucleus, calculated by us for the K2 potential with non-point nucleons is shown in Fig. 8 together with the corresponding experimental data [17]. It can be seen that the result fits well the experimental data in the region before the “dip”. The agreement is worse after the dip. It should be mentioned that, in the region of large momentum transfer (small distances, respectively), our consideration of non-point nucleons adiabatically in

the form (25) is insufficient. It is possible, for example, to use the adiabatic formula (25) before the first “dip” (relatively large distances) and then, after the “dip” (in region of small distances), to treat nucleons as point-like particles, because there is no sense to use the adiabatic approach (non-point nucleons strongly overlap one another). Within such assumptions, the theoretical formfactors better fit the experiment. The formfactor calculated by us has also a good agreement with the other experiment [21]. For a T nucleus, everything is the same.

It is interesting to examine the properties of the “dip” in the formfactor. The position of this “dip” is connected directly with properties of the short-range interaction between nucleons. For a purely attractive potential, the formfactor of a three-nucleon system has no “dip” at all. With the appearance and increase of the repulsion, the “dip” appears in the region of large q^2 and then moves left (approaches the experimental position). The essential repulsion in the K2 potential puts the charge formfactor of a nucleus (for example, ${}^3\text{He}$) very close to the experimental data. One can expect that some greater increase of the repulsion in the nuclear interaction potential will be sufficient for a full agreement with the experimental data on charge formfactors. Since the formfactors are connected with charge distributions, we can mention that the position of the formfactor “dip” directly depends on a short-range irregularity, which, in its turn, depends on the repulsion part of the NN-potential.

We note that the formfactors can have other “dips” at larger q^2 . The number of “dips” depends on the form and the intensity of short-range repulsion in potentials as well as on the accuracy of calculations and the dimension of a Gaussian basis. There are some calculational difficulties for the Gaussian representation of wave functions during the description of the asymptotic behavior of formfactors at very large q^2 .

7. Conclusions

The potential of nucleon-nucleon interaction is constructed in a simple form (K2) for the simultaneous description of low-energy two-nucleon experimental data and the binding energies of a deuteron, triton, ${}^3\text{He}$, and ${}^4\text{He}$. The binding energies of three- and four-nucleon nuclei are calculated with high precision for different potentials using the representation without isospin and variational methods with Gaussian bases. The density distributions and the formfactors of nuclei T and ${}^3\text{He}$ for the K2 potential are calculated, and their agreement

with experimental data is discussed. The presence of some irregularity in the density behavior and the dependence of the position of a “dip” in the formfactor on the short-range potential behavior are revealed. The wave functions of three-nucleon systems obtained in the convenient form can be used in the examination of other structure functions, such as the pair correlation functions and the momentum distributions. This will be done in our next work. The proposed simple potentials also can be used for the analysis of scattering processes including few-nucleon systems.

1. V.I. Kukulín and V.M. Krasnopol'sky, *J. Phys. G: Nucl. Phys.* **3**, 795 (1977).
2. N.N. Kolesnikov and V.I. Tarasov, *Yad. Fiz.* **35**, 609 (1982).
3. K. Varga and Y. Suzuki, *Phys. Rev. C* **52**, 2885 (1995).
4. I.V. Simenog, I.S. Dotsenko, and B.E. Grinyuk, *Ukr. Fiz. Zh.* **47**, 129 (2002).
5. R. Lazauskas, Ecole Doctorale de Physique. These: *Etude de la diffusion de particules lourdes sur des systemes atomiques et nucleaires*, 2003, Universite Joseph Fourier-Grenoble I, France.
6. B.E. Grinyuk, D.V. Piatnytskyi, and I.V. Simenog, *Ukr. Fiz. Zh.* **52**, 424 (2007).
7. V.G.J. Stoks, R.A.M. Klomp, C.P.F. Terheggen, and J.J. de Swart, *Phys. Rev. C* **49**, 2950 (1994).
8. R.B. Wiringa, V.G.J. Stoks, and R. Schiavilla, *Phys. Rev. C* **51**, 38 (1991).
9. R. Machleidt, F. Sammarruca, and Y. Song, *Phys. Rev. C* **53**, 1483 (1996).
10. B.E. Grinyuk and I.V. Simenog, *Ukr. Fiz. Zh.* **45**, 625 (2000).
11. V.V. Babikov, *The Variable Phase Approach in Quantum Mechanics* (Nauka, Moscow, 1976) (in Russian).
12. R. Machleidt, *Phys. Rev. C* **63**, 024001 (2001).
13. A.H. Wapstra and G. Audi, *Nucl. Phys.* **A432**, 1 (1985).
14. R.C. Barret and D.F. Jackson, *Nuclear Sizes and Structure* (Clarendon Press, Oxford, 1977).
15. R.F. Frosch *et al.*, *Phys. Rev.* **160**, 874 (1967).
16. C.R. Ottermann *et al.*, *Nucl. Phys.* **A436**, 688 (1985).
17. J.S. McCarthy, I. Sick, and R.R. Whitney. *Phys. Rev. C* **15**, 1396 (1977).
18. Z.M. Szalata *et al.*, *Phys. Rev. C* **15**, 1200 (1977).
19. P.C. Dunn *et al.*, *Phys. Rev. C* **27**, 71 (1983).
20. F.-P. Juster *et al.*, *Phys. Rev. Lett.* **55**, 2261 (1985).
21. A. Amroun *et al.*, *Nucl. Phys.* **A579**, 596 (1994).
22. A.I. Akhiezer, A.G. Sitenko, and V.K. Tartakovsky, *Nuclear Electrodynamics* (Springer, Berlin, 1994).

Received 28.11.07

ЯДЕРНІ ПОТЕНЦІАЛИ ВЗАЄМОДІЇ ДЛЯ СУМІСНОГО ОПИСУ МАЛОНУКЛОННИХ СИСТЕМ І СТРУКТУРНІ ФУНКЦІЇ ТРИНУКЛОННИХ ЯДЕР

Д.В. П'ятницький, І.В. Симоног

Резюме

Запропоновано варіант потенціалу нуклон-нуклонної взаємодії, який задовільно узгоджує опис низькоенергетичних параметрів двох нуклонів і енергій три- та чотиринуклонних ядер. Описана схема конструювання таких потенціалів взаємодії. Виконано розрахунок з високою точністю енергій зв'язку та розмірів три- та чотиринуклонних ядер в рамках варіаційного методу з оптимізованим гаусоїдним базисом з різними потенціалами взаємодії, де використано переваги представлення без ізоспіну. Проаналізовано поведінку структурних функцій ядер Т та ^3He .